

Michael S. Salman
Susan E. Blaser
James A. Sharpe
Maureen Dennis

Cerebellar vermis morphology in children with spina bifida and Chiari type II malformation

Received: 21 January 2005
Revised: 23 February 2005
Published online: 22 December 2005
© Springer-Verlag 2005

M. S. Salman
Division of Neurology,
The Hospital for Sick Children,
Toronto, Canada

M. S. Salman · J. A. Sharpe
Division of Neurology,
Toronto Western Hospital,
University of Toronto,
Toronto, Canada

M. S. Salman (✉)
Section of Paediatric Neurology,
AE 108, Harry Medovy House,
Children's Hospital,
820 Sherbrook Street,
Winnipeg, Manitoba, R3A 1R9,
Canada
e-mail: msalman@hsc.mb.ca
Tel.: +1-204-7872414
Fax: +1-204-7871922

S. E. Blaser
Division Radiology,
The Hospital for Sick Children,
Toronto, Canada

M. Dennis
Division Psychology,
The Hospital for Sick Children,
Toronto, Canada

Abstract Objective: Posterior fossa size and cerebellar weight and volume are reduced in Chiari type II malformation (CII). This is assumed to affect the cerebellum uniformly. We quantified the presumed reduction in vermis size on magnetic resonance imaging (MRI). **Methods:** A midsagittal brain MRI slice was selected from each of 68 participants with CII (mean age 13 years). Control participants were 28 typically devel-

oping children (mean age 14.1 years). Midsagittal surface areas occupied by the intracranial fossa, posterior fossa, vermis, and its lobules were measured. **Conclusions:** Mean posterior fossa area was significantly smaller ($P<0.003$), although mean vermis area was significantly larger ($P<0.0001$), in participants with CII than in control participants. This expansion involved vermis lobules I–V and VI–VII areas ($P<0.0001$). The midsagittal vermis was expanded and not reduced in size in participants with CII. This is attributed to compressive displacement of midline structures within the confines of a small posterior fossa.

Keywords Cerebellar malformation · Vermis morphology · Children · Spina bifida · MRI · Midsagittal area

Introduction

Chiari type II malformation (CII) is a congenital developmental anomaly of the brainstem and cerebellum [7]. The most widely accepted theory proposes that the crowding of a small posterior fossa is responsible for CII [22]. Cerebellar volume, weight, and cell content are reduced in CII [5, 6, 11, 12, 15, 16, 28, 36, 41]. The small cerebellar size has been blamed on mechanical compression, secondary to crowding, which is presumed to lead to secondary ischemic changes and parenchymal cerebellar loss [5]. Measuring regional morphological variations in CII is challenging and has not been performed systematically. The dysmorphology of the hindbrain makes the identification of many of the anatomical markers difficult. The borders between the

vermis and the cerebellar hemispheres are blurred and are hard to delineate with any certainty, making volumetric measurements of the vermis in CII unreliable. Furthermore, wide variation in CII deformity has been reported on shape analyses in subjects with CII [39]. Thus, positioning any markers across different scans for the purpose of averaging them for volumetric analysis is also difficult. Measuring areas of different regions of interest, also known as planimetry, can provide information about specific brain regions. Planimetry of the posterior fossa and herniation distance below the foramen magnum has been reported in 25 subjects with CII [39].

In this study, structures within the posterior fossa were identified on high-quality magnetic resonance imaging (MRI) scans of children with CII and of typically developing con-

trols. Our aim was to confirm the presence of vermis lobules in CII and to measure the distances and areas of various regions of interest in CII and compare them with measurements from control participants, to quantify the presumed reduction in vermis size associated with CII. The effects of age, gender, and spinal lesion level on these MRI measurements were also investigated.

Materials and methods

Participants

Participants were selected from a cohort of patients and controls who were participants in a spina bifida project funded by the National Institute of Child Health and Human Development. The study was approved by the Hospital for Sick Children (HSC) Research Ethics Board. All participants had brain MRI scans that were artifact-free. Sixty-eight of the participants had myelomeningocele and CII, eight of which had posterior fossa decompression surgery. Spinal lesion level was obtained from their medical charts, parent's interview, or MRI scans of the brain and spine. Two groups were distinguished: upper spinal lesion level group [thoracic vertebrae 12 (T12) and above] and lower spinal lesion level group [lumbar vertebrae 1 (L1) and

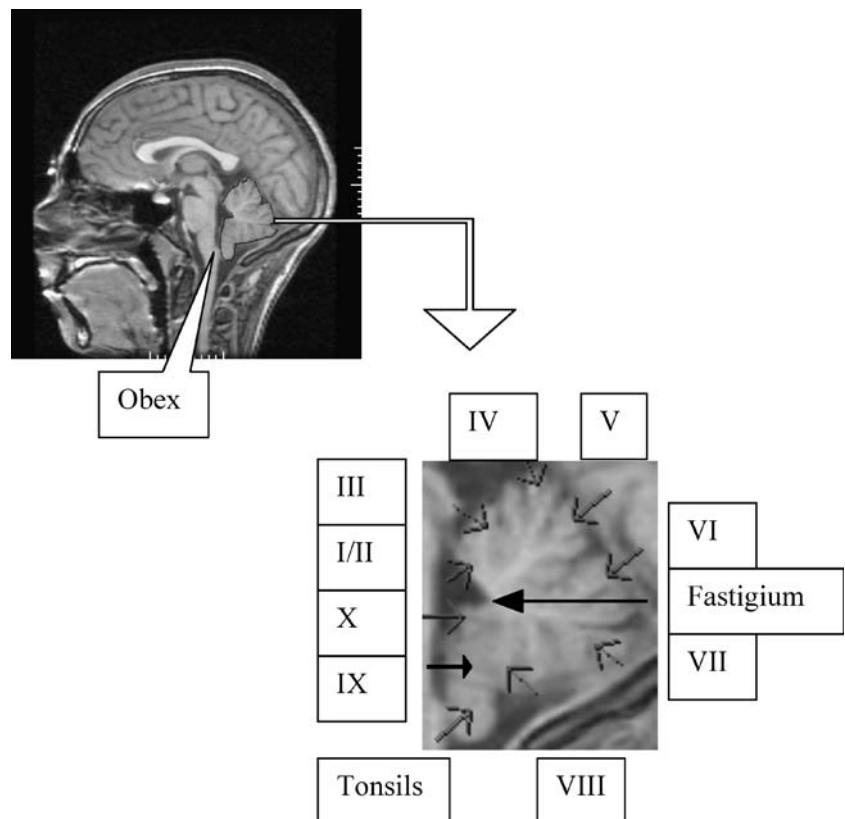
below], based on the developmental process of the neural tube closure [40]. Twenty-eight participants were typically developing children; they constituted the control group.

Brain imaging procedure

MRI images were acquired on a 1.5-T GE MRI scanner. Three sets of images were obtained, and the techniques have been described in detail elsewhere [11]. The brain MRI images were displayed using the Pathspeed Workstation 8.1, GE, 1998. The following posterior fossa structures were identified with the aid of *MRI Atlas of the Human Cerebellum* [34]: ten cerebellar vermis lobules and the superior and inferior medullary veli on midsagittal brain MRI. In addition, axial and coronal images were used to identify the tonsils and flocculus and to determine whether herniation below the foramen magnum was present.

The distances and the areas of regions of interest were measured using a specialized software (Ataman Software Inc., 1998) on T1- or T2-weighted midsagittal MRI images. The midsagittal MRI image was selected using three or more of the following landmarks: aqueduct of Sylvius, obex, and III and IV ventricles (Fig. 1). Midsagittal MRI image provided consistency across all subjects despite the deformity of CII. One investigator (MSS) performed all measure-

Fig. 1 Midsagittal T1-weighted brain MRI illustrating the obex and the cerebellar vermis. The vermis cerebellar lobules are identified by *Roman numerals*



ments. Two sets of measurements of MRI parameters were done on each scan over few sessions (5–10 scans per session), except for herniation distance, which was measured once. The following parameters were used as markers for intracranial and cerebellar dysmorphology in CII (Figs. 2 and 3):

1. The longest longitudinal distance across the vermis
2. The longest transverse distance across the vermis, defined as a line passing through the vermis and joining the posterior tip of the IV ventricle (fastigium) and the most posterior part of the vermis
3. Herniation distance and the area below the foramen magnum
4. Intracranial fossa, delineated by a line passing through the opisthion (posterior part of foramen magnum), basion (anterior part of foramen magnum), anterior border of the brainstem, posterior part of the floor of the pituitary fossa, roof of the pituitary fossa, cerebral cortex, torcula, border of the posterior part of the skull, and opisthion
5. Posterior fossa area, delineated by a line passing through the opisthion, basion, anterior border of the brainstem, posterior part of the floor of the pituitary fossa, border between the superior and inferior colliculi, roof of the vermis, border of the posterior part of the skull, and opisthion
6. Cerebellar vermis
7. Vermis lobules I–V, and
8. Vermis lobules VI–VII

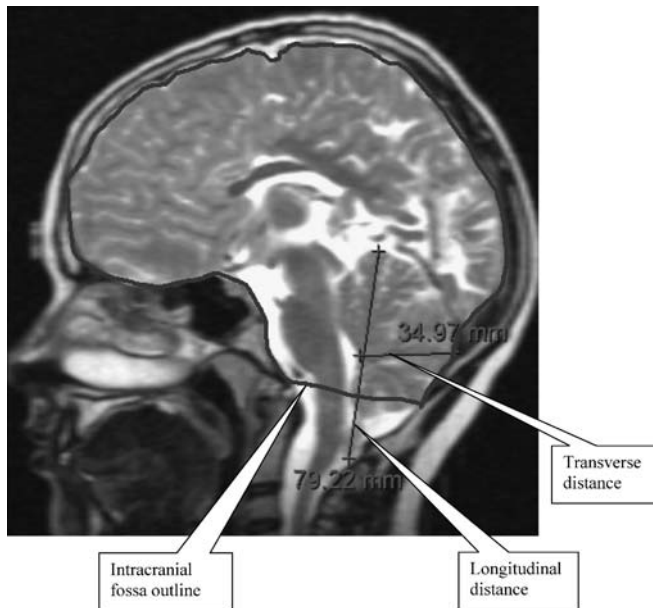


Fig. 2 Midsagittal T2-weighted brain MRI of a child with Chiari malformation illustrating intracranial fossa borders and longitudinal and transverse distances across the cerebellar vermis

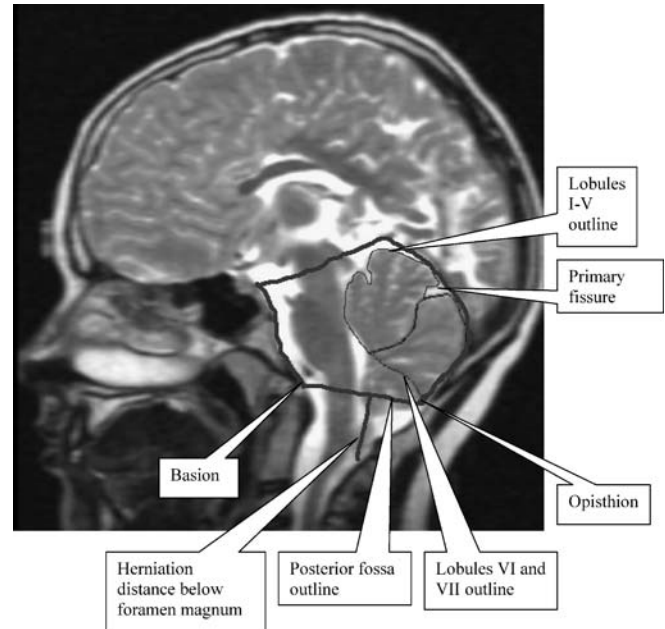


Fig. 3 Midsagittal T2-weighted brain MRI of a child with Chiari malformation illustrating the borders of the posterior fossa, cerebellar vermis lobules, and herniation distance below foramen magnum

Analyses

A Statistical Package for Social Sciences (SPSS) software was used to set up a database for analyses [38]. To assess the reliability of measurements, 20 MRI scans (11 with CII) were selected randomly and independently by a technologist blinded to the purpose of the study. The technologist measured the same MRI parameters independently, and these measurements were compared with the investigator's (MSS) mean measurements using a scatter diagram to evaluate interobserver reliability [1]. If the two measurements agreed, then the points would be expected to lie on the line of equality, which is the gradient (G) of the best line fit. In addition, the differences between the values that were measured by the investigator and by the technologist were plotted against their average values. This plot allows for the size of the differences to be seen more easily, in addition to their distributions around zero [1]. To evaluate intraobserver reliability, the two measurements obtained by the investigator for each parameter were analyzed by the same methods for interobserver reliability.

Descriptive data Data were compared using two-tailed independent Student t tests for continuous variables (e.g., age) and the chi-squared test or Fisher's exact test for categorical variables (e.g., proportion of participants in whom the cerebellar flocculus could be identified on MRI scan). Significance was defined as $P < 0.05$. The normality of data distribution was tested using the mean, median, standard deviation (SD), skewness, kurtosis, and box plots.

Bivariate comparisons Two types of analyses were done. The first was a set of two-tailed, independent Student *t* tests between the control and CII groups to investigate group differences. Because multiple comparisons are more likely to yield apparently significant results, Bonferroni adjustment was applied [23]. A *P* value of <0.01 was required to achieve statistical significance. The second type of analyses was done within the control and CII groups to investigate the effect of gender. In addition, further variability in the CII group was investigated based on spinal lesion level and whether participants had posterior fossa decompression surgery. Such surgery could alter MRI measurements. The location of the opisthion in those patients was estimated with the aid of coronal MRI sections and brain MRI images prior to the surgical decompression. Two-tailed independent Student's *t* tests were used for the analyses. Age was correlated with MRI data in each group using two-tailed Spearman correlation tests.

Results

MRI measurements were completed in all scans, except for one intracranial fossa area and two lobules I–V and VI–VII areas in two participants with CII because of inadequate MRI views due to technical reasons. The participants' demographics were comparable (Table 1). Fifty-one participants

with CII had lower spinal lesion level (L1 and below), and 17 had upper spinal level lesion (T12 and above). The distribution of the MRI data was approximately normal.

Identification of the cerebellar lobules

The percentages of participants in whom vermis lobules and other posterior fossa structures were identified are presented in Table 1. The nodulus (lobule X) and flocculus were significantly less likely to be identifiable in the CII group than in the control group.

Interobserver variability There was good agreement in the MRI measurements performed by the investigator and technologist for most measurements (Table 2). Poor concordance in two measurements was noted. The first was the vermis lobules VI–VII area in the control group due to the erroneous inclusion of part of the cerebellar hemisphere that protruded onto the midsagittal MRI scan in one participant. The second was in the herniation area below the foramen magnum in the CII group because one participant had CII decompression surgery that left a scar tissue and blurred the border of the herniated area. Therefore, two out of 180 measurements were not concordant, i.e., ~1% error in a total of nine measurements in each of the 20 participants. In plots showing the difference in the two measurements against their average value (not shown), the distribution was random overall and centered close to zero, except for the plots showing the two outlying values mentioned above.

Intraobserver variability There was good agreement between the two MRI measurements performed by the investigator for most parameters (Table 2). In plots showing the difference in the two measurements against their average value (not shown), the distribution was random overall and centered close to zero.

Table 1 Demographic data and number of participants (%) in whom cerebellar structures were identified on MRI

	Control group	CII ^a group	<i>P</i> value ^b
Number of participants	28	68	
Gender	13 Females	37 Females	
Age range, mean, SD (years)	8–19, 14.1, 3.1	8–19, 13.0, 3.1	
Vermis lobules I and II	27 (96.4)	59 (86.8)	0.27
Vermis lobule III	28 (100)	65 (95.6)	0.55
Vermis lobules IV and V	28 (100)	66 (97.1)	1.00
Vermis lobule VI	28 (100)	66 (97.1)	1.00
Vermis lobule VII	28 (100)	66 (97.1)	1.00
Vermis lobule VIII	28 (100)	63 (92.6)	0.32
Vermis lobule IX	28 (100)	63 (92.6)	0.32
Vermis lobule X	28 (100)	56 (82.4)	0.02*
Cerebellar tonsils	28 (100)	67 (98.5)	1.00
Flocculus	28 (100)	58 (85.3)	0.03*
Superior medullary velum	28 (100)	65 (95.6)	0.55
Inferior medullary velum	28 (100)	64 (94.1)	0.32

^aChiari type II

^bSignificance is defined at *P*<0.05 on chi-squared test

Differences between groups

There was a significant difference in all MRI parameters by group, except for the mean intracranial fossa area (*P*=0.023; Fig. 4). The mean posterior fossa area was smaller in participants with CII than in controls (*P*=0.003). However, mean vermis area, means of the longest transverse, and longitudinal distances across the vermis were larger in participants with CII than in controls (*P*<0.0001). All vermis lobule mean areas were larger in participants with CII than in controls (*P*<0.0001; Fig. 4). The results remained significant after adjusting for variation in intracranial fossa area. Vermis herniation distance below the foramen magnum in participants with CII had a mean of 17 mm (range 5.2–44.2 mm). None of the controls had herniation.

Table 2 Inter- and intraobserver reliability data

MRI data	Interobserver data				Intraobserver data			
	Control group		CII group		Control group		CII group	
	G^a	R^{2b}	G	R^2	G	R^2	G	R^2
Transverse distance	0.86	0.96	0.79	0.91	1.02	0.97	0.96	0.94
Longitudinal distance	0.92	0.97	0.85	0.71	0.98	0.98	0.98	0.99
Herniation distance	1.0 ^c	–	1.04	0.96	NA	NA	ND	ND
Intracranial area	1.07	0.98	0.98	0.93	1.00	0.99	1.00	1.00
Posterior fossa area	0.69	0.80	1.07	0.76	0.97	0.96	0.98	0.99
Cerebellar vermis/tonsil area	1.07	0.88	0.89	0.82	0.99	0.99	1.00	0.99
Vermis lobules I–V area	1.33	0.80	0.79	0.81	0.90	0.96	0.98	0.98
Vermis lobules VI–VII area	0.14 ^d	0.01	1.06	0.95	1.02	0.86	1.03	0.96
Herniation area	1.0 ^c	–	0.45 ^d	0.80	NA	NA	0.98	0.98

The gradient and variance values of the linear equation fitted through the MRI data are shown, *NA* not applicable, *ND* not done because it was measured once

^aGradient

^bVariance

^cThe technologist and the investigator (MSS) agreed that there was no herniation in any participant in the control group

^dPoor concordance-see [Results](#) for explanation

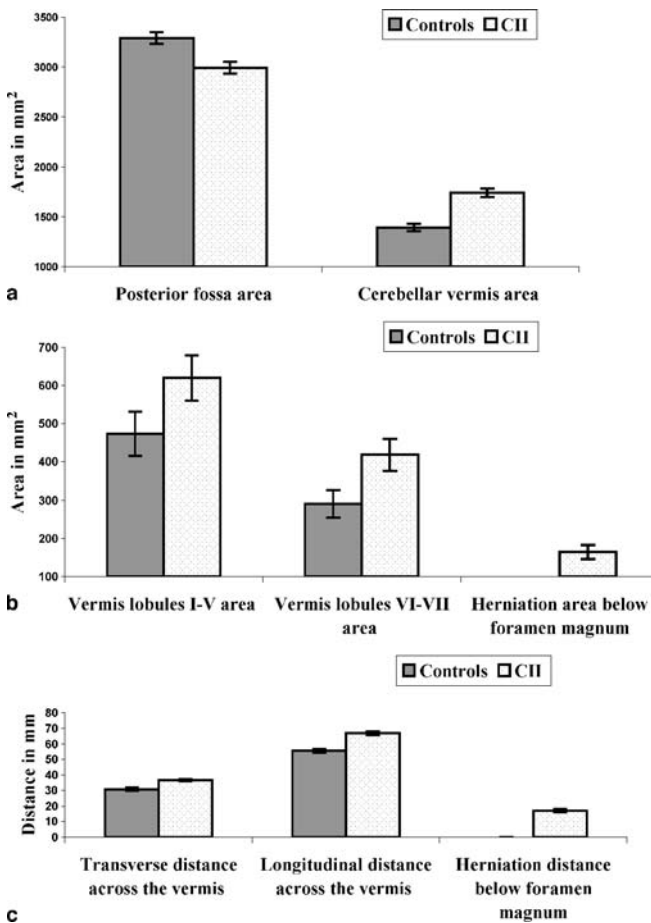


Fig. 4 MRI measurements in the control and CII groups on midsagittal MRI. **a** Mean areas of the posterior fossa and vermis (± 1 SE) in square millimeters. **b** Mean areas of vermis lobules and herniation area (± 1 SE) in square millimeters. **c** Mean longest transverse and longitudinal distances across the vermis, and mean herniation distance below foramen magnum (± 1 SE) in millimeters

Variability in the control group

Older participants had larger intracranial fossa [Spearman's correlation coefficient (ρ)=0.443, $P=0.018$] and posterior fossa ($\rho=0.412$, $P=0.029$) areas. Compared with boys, girls had a significantly smaller mean posterior fossa area (3,131 vs 3,430 mm² in boys, $P=0.008$) and smaller mean intracranial fossa area (14,958 vs 15,777 mm² in boys, $P=0.058$) and mean vermis lobules I–V area (446.1 vs 496.1 mm² in boys, $P=0.043$).

Variability in the CII group

Age did not correlate with any of the MRI measurements. Girls had significantly smaller mean intracranial fossa area (15,643 vs 16,665 mm² in boys, $P=0.003$), mean herniation distance (14.7 vs 19.9 mm² in boys, $P=0.006$), and mean herniation area below the foramen magnum (131.9 vs 203.1 mm² in boys, $P=0.003$) than boys did. Girls also had a shorter mean of the longest transverse (35.4 vs 38.4 mm in boys, $P=0.024$), longitudinal distances across the vermis (65 vs 69.5 mm in boys, $P=0.038$), mean vermis area (1,662 vs 1,833 mm² in boys, $P=0.041$), and mean vermis lobules VI–VII area (395.3 vs 446.3 mm² in boys, $P=0.052$) than boys did.

There were no significant differences in MRI measurements by spinal lesion level. However, there was a trend for the mean posterior fossa area (2,796 mm²), mean vermis area (1,572 mm²), and mean vermis lobules I–V area (544.6 mm²) of the upper spinal lesion level group ($N=17$) to be smaller compared with the mean posterior fossa area (3,059 mm², $P=0.053$, $N=51$), mean vermis area (1,796 mm², $P=0.019$, $N=51$), and mean vermis lobules I–V area (646 mm², $P=0.014$, $N=49$) of the lower spinal lesion level group.

Table 3 Studies in which planimetry of brain regions was performed (mean or range in mm²) on midsagittal MRI in typically developing children

Reference	Number/ gender ^a	Mean age (SD), range [years]	Intracranial fossa	Posterior fossa	Cerebellar vermis	Vermis lobules I–V	Vermis lobules VI–VII	Vermis lobules VIII–X
Murakami et al., 1989 [26]	8	28.3, 19–37	NA	NA	NA	394	271	NA
Jernigan et al., 1990 [18]	9	8–10	NA	NA	NA	430–620	270–360	NA
Aylward et al., 1991 [2]	20 M	12.5, 1–32	NA	NA	850–1,300	NA	NA	NA
Shah et al., 1991 [37]	16 M 20 F	36.6 (10) 26–79	NA	NA	1,160 1,160	483 490	← 672 → ← 670 →	
Raz et al., 1992 [30]	29	43.6 (17.8), 18–78	18,321	NA	965	403	252	310
Courchesne et al., 1994 [9]	53	18.8, 3–37	NA	NA	NA	426.6	282.2	NA
Saitoh et al., 1995 [33]	23	13.3 (8.1)	NA	NA	NA	NA	279.4	NA
Jacobsen et al., 1997 [17]	28 M 24 F	14.3 (2)	NA	NA	NA	501 472.2	304.4 315.1	361.9 343.2
Piven et al., 1997 [29]	36	20.2 (3.8)	NA	NA	NA	500	310	NA
Berquin et al., 1998 [4]	47 M	11.8 (3)	NA	NA	1,030	502	309	356
Lesnik et al., 1998 [20]	10	6–13	NA	NA	NA	425.5	322.7	NA
Mostofsky et al., 1998 [24]	38 M 53 F	12.5, 1–44 11.3, 3–26	15,882 15,010	NA	1,153 1,100	482 454	314 322	357 323
Mostofsky et al., 1998 [25]	23 M	11.3, 6.6–24.6	16,287	NA	1,226	512	326	389
Raz et al., 1998 [31]	146	46.6 (17.4), 18–77	NA	NA	NA	341	231	306
Christophe and Dan, 1999 [8]	43	5.4 ^b , 0.04–17	NA	2,800–3,800 for >8 years old	1,061 ^b (1,000–1,500 for >8 years old)	NA	NA	NA
Levitt et al., 1999 [21]	21	12 (2.8), 7.9–16.8	NA	NA	NA	NA	NA	281.8
Nopoulos et al., 1999 [27]	65 M	27.2 (5.9), 18–44			1,189	500	315	373
Courchesne et al., 2001 [10]	52 M	2–16	NA	NA	NA	NA	291	NA
Hardan et al., 2001 [14]	22	22.4 (10), 12.9–52.2	NA	NA	1,040	440	270	340
Schmitt et al., 2001 [35]	20	28.5 (8.2), 19–48	15,830	NA	1,264	541	372	372
Tsai et al., 2002 [39]	25	2–35	NA	2,871.7	NA	NA	NA	NA
Salman et al., current study	28	14.1 (3.1), 8–19	15,397	3,291	1,391	473	291	627 ^c

^aNumber/gender: number of participants/males (M), females (F)^bMedian value^cThis measurement includes the cerebellar tonsils and was obtained by subtracting the areas of vermis lobules I–IV and VI–VII from cerebellar vermis/tonsil area. This was done to compare our results with other published values

There was no significant difference in the MRI parameters between participants with CII who had posterior fossa decompression surgery compared with participants who did not have this surgery.

Discussion

The cerebellum is nonuniformly affected in CII. Although the posterior fossa has a small midsagittal area in CII, the midsagittal cerebellar vermis occupies a larger part of it in the participants with CII than in the controls. The main issues discussed are vermis lobules in CII, quantification of the cerebellar dysmorphology of CII on midsagittal brain MRI, and variations of the MRI measurements with age, gender, and spinal lesion level.

In CII, the vermis lobules can be identified on MRI. The results of this investigation are consistent with the proposal that CII is a manifestation of a crowded posterior fossa [16, 22]. The distortion of posterior fossa contents made the identification of the nodulus (vermis lobule X) and flocculi (the bihemispheric extensions of the nodulus) more difficult.

The deformity of the cerebellum in CII makes volumetric quantification of the vermis on MRI challenging because the borders between the vermis and the cerebellar hemispheres cannot be delineated reliably. Planimetry of midsagittal MRI images offers a simple and reproducible method to study the vermis noninvasively. Its intra- and interobserver reliabilities are evident in this investigation. Normal values of regions of interest in this study are in agreement with many studies after taking age into account (Table 3).

This investigation has shown, for the first time, a significant increase in vermis area in CII despite a smaller posterior fossa area on midsagittal MRI compared with the normal vermis. This increase involves longitudinal and transverse expansion of the vermis. A small posterior fossa size in CII has been reported in other studies [3, 6, 16, 22, 39]. The landmark used to delineate the upper border of the posterior fossa in this study may have underestimated the magnitude of the reduction in posterior fossa size in CII. We used the upper border of the cerebellum, which normally conforms to the location of the tentorium; however, in CII, the cerebellum may herniate upward through an enlarged incisural notch [19].

Planimetry and distance measurements on midsagittal MRI do not provide a global view of the vermis changes that are associated with CII. Nevertheless, area changes in the midline vermis add information to the sparse existing knowledge in this area.

Overall cerebellar size is reduced in CII [5, 6, 11, 12, 15, 16, 28, 36, 41]. The number of cells and DNA content in the internal granular layer of the vermis are reduced, more so in the inferior lobules than in the central lobules in CII [12]. Cerebellar weights are reduced in neonates with CII

[41]. The herniated cerebellar tissue in CII shows Purkinje and granule cell depletion, shrinkage and gliosis of the folia, and myelin depletion [15]. MRI volumetric analysis [11] has revealed reduced cerebellar volumes involving both the gray and white matter in CII and that the reduction in cerebellar volume was greater in children with high spinal lesion levels than in those with low spinal lesion levels. Findings from the current investigation suggest that the reported reduction in cerebellum volume is not uniform and likely involves the cerebellar hemispheres, which have no place for expansion and growth within the confines of small posterior fossa. However, the vermis may be less affected than the cerebellar hemispheres in CII because, being a midline structure, the vermis can expand rostrally [19], caudally through foramen magnum [19], and in a ventral–dorsal direction. In other words, major midsagittal crowding is apparent in CII.

A larger midsagittal vermis area might result from hypertrophy or hyperplasia of the vermis. This is unlikely, however, because some studies have reported a smaller overall cerebellar size and cellular content in CII [12, 15]. The likely explanation for an enlarged midsagittal vermis area is mechanical pressure that results from a small and crowded posterior fossa. This pressure generates forces that squeeze the vermis from either side towards the midline, resulting in the apparent increase in its surface area on midsagittal MRI (Fig. 5). This proposed mechanism could be investigated further by anatomical study of the cerebellar vermis in CII. All vermis lobule areas were larger in participants with CII than in controls. Therefore, the increase in the entire vermis area cannot be explained by inferior vermis herniation. The trend for larger mean intracranial fossa area in the CII group despite a smaller posterior fossa area in comparison with the controls is attributed to the hydrocephalus associated with CII.

A modest effect of age on the intracranial and posterior fossa areas was noted in the control group in this investi-

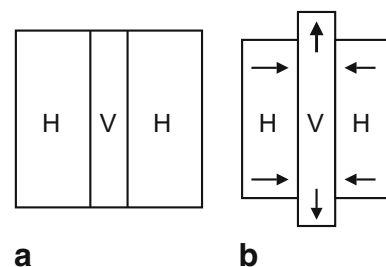


Fig. 5 Model for the morphological change of the cerebellum in CII. The diagrams (not drawn to scale) illustrate a coronal section through the cerebellar hemispheres (*H*) and vermis (*V*) in a control (**a**) and in an individual with CII (**b**). The arrows in **b** depict the change in CII. The width of the vermis is reduced secondary to compression by the cerebellar hemispheres, but its midsagittal size is larger in participants with CII than in controls. The size of the cerebellar hemispheres is reduced. Current evidence supports this model

gation, reflecting brain growth [32]. Gender difference in brain size [32] was confirmed in this investigation.

There was a trend for a smaller posterior fossa in the upper spinal lesion level group. Upper spinal lesions in spina bifida are a marker of more severe brain dysmorphology and are associated with poorer cognitive and behavioral outcomes [13].

Conclusions

This investigation has shown, for the first time, that the cerebellum is nonuniformly affected in CII. Although the posterior fossa has a small midsagittal area in CII, the cerebellar vermis occupies a larger part of it in the participants

with CII than in the controls. This increase in vermis area involves all vermis lobules on midsagittal MRI. This finding may have implications on regional cerebellar function.

Acknowledgements We thank Drs. Daune L. MacGregor, Teresa To, and Pheroze Bharucha, Miss Dawn Greer, and Mrs. Irit Dror for their help and support. Financial support: (1) Research training competition award, The HSC; (2) KidsAction; (3) Spina Bifida and Hydrocephalus Association of Canada; (4) Clinician Scientist training program awards, HSC, and Vision Science Research Program at Toronto Western Hospital; (5) Bloorview MacMillan Hospital foundation grants (MS Salman); (6) National Institutes of Health grant (J Fletcher, M Dennis) "Spina bifida: Cognitive and neurobiological variability"; and (7) Canadian Institute of Health Research of Canada grants MT5404 and ME 5909 (JA Sharpe).

References

- Altman DG (1995) Practical statistics for medical research. Chapman & Hall, London
- Aylward EH, Reiss A (1991) Area and volume measurement of posterior fossa structures in MRI. *J Psychiatr Res* 25:159–168
- Barkovich AJ (2000) Congenital malformations of the brain and skull/congenital anomalies of the spine. In: Barkovich AJ (ed) *Pediatric neuroimaging*. Lippincott Williams & Wilkins, Philadelphia, PA, pp 330–337
- Berquin PC, Giedd JN, Jacobsen LK, Hamburger SD, Krain SL, Rapoport JL, Castellanos FX (1998) Cerebellum in attention-deficit hyperactivity disorder: a morphometric MRI study. *Neurology* 50:1087–1093
- Boltshauser E, Schneider J, Kollias S, Waibel P, Weissert M (2002) Vanishing cerebellum in myelomeningocele. *Eur J Paediatr Neurol* 6:109–113
- Brocklehurst G (1969) A quantitative study of a spina bifida foetus. *J Pathol* 99:205–211
- Chiari H (1891) Ueber Veraenderungen des Kleinhirns infolge von Hydrocephalie des Grosshirns. *Dtsch Med Wochenschr* 17:1172–1175
- Christophe C, Dan B (1999) Magnetic resonance imaging cranial and cerebral dimensions: is there a relationship with Chiari I malformation? A preliminary report in children. *Eur J Paediatr Neurol* 3:15–23
- Courchesne E, Saitoh O, Yeung-Courchesne R, Press GA, Lincoln AJ, Haas RH, Schreibman L (1994) Abnormality of cerebellar vermis lobules VI and VII in patients with infantile autism: identification of hypoplastic and hyperplastic subgroups with MR imaging. *Am J Roentgenol* 162:123–130
- Courchesne E, Karns CM, Davis HR, Ziccardi R, Carper RA, Tigue ZD, Chisum HJ, Moses P, Pierce K, Lord C, Lincoln AJ, Pizzo S, Schreibman L, Haas RH, Akshoomoff NA, Courchesne RY (2001) Unusual brain growth patterns in early life in patients with autistic disorder: an MRI study. *Neurology* 57:245–254
- Dennis M, Edelstein K, Hetherington R, Copeland K, Frederick J, Blaser SE, Kramer LA, Drake JM, Brandt M, Fletcher JM (2004) Neurobiology of perceptual and motor timing in children with spina bifida in relation to cerebellar volume. *Brain* 127:1–10
- Emery JL, Gadsdon DR (1975) A quantitative study of the cell population of the cerebellum in children with myelomeningocele. *Dev Med Child Neurol* 15(Suppl 29):20–25
- Fletcher JM, Copeland K, Frederick JA, Blaser SE, Kramer LA, Northrup H, Hannay HJ, Brandt ME, Francis DJ, Villarreal G, Drake JM, Laurent JP, Townsend I, Inwood S, Boudousquie A, Dennis M (2005) Spinal lesion level in spina bifida: a source of neural and cognitive heterogeneity. *J Neurosurg* 102:268–279
- Hardan AY, Minshew NJ, Harenski K, Keshavan MS (2001) Posterior fossa magnetic resonance imaging in autism. *J Am Acad Child Adolesc Psych* 40:666–672
- Harding BN, Copp AJ (2002) Malformations. In: Graham DI, Lantos PL (eds) *Greenfield's neuropathology*. Edward Arnold, London, pp 376–386
- Hori A (2002) Chiari anomaly type II without cerebellar herniation. *Acta Neuropathol* 105:193–194
- Jacobsen LK, Giedd JN, Berquin PC, Krain AL, Hamburger SD, Kumra S, Rapoport JL (1997) Quantitative morphology of the cerebellum and fourth ventricle in childhood-onset schizophrenia. *Am J Psychiatry* 154:1663–1669
- Jernigan TL, Tallal P (1990) Late childhood changes in brain morphology observable with MRI. *Dev Med Child Neurol* 32:379–385
- Just M, Schwarz M, Ludwig B, Erment J, Thelen M (1990) Cerebral and spinal MR—findings in patients with postrepair myelomeningocele. *Pediatr Radiol* 20:262–266
- Lesnik PG, Ciesielski KT, Hart BL, Benzel EC, Sanders JA (1998) Evidence for cerebellar-frontal subsystem changes in children treated with intrathecal chemotherapy for leukemia: enhanced data analysis using an effect size model. *Arch Neurol* 55:1561–1568
- Levitt JG, Blanton R, Capetillo-Cunliffe L, Guthrie D, Toga A, McCracken JT (1999) Cerebellar vermis lobules VIII–X in autism. *Prog Neuropsychopharmacol Biol Psychiatry* 23:625–633

22. McLone DG, Knepper PA (1989) The cause of Chiari II malformation: a unified theory. *Pediatr Neurosci* 15:1–12
23. Miller RG (1981) *Simultaneous statistical inference*. Springer, Berlin Heidelberg New York, pp 6–8
24. Mostofsky SH, Mazzocco MM, Aakalu G, Warsofsky IS, Denckla MB, Reiss AL (1998) Decreased cerebellar posterior vermis size in fragile X syndrome: correlation with neurocognitive performance. *Neurology* 50:121–130
25. Mostofsky SH, Reiss AL, Lockhart P, Denckla MB (1998) Evaluation of cerebellar size in attention-deficit hyperactivity disorder. *J Child Neurol* 13:434–439
26. Murakami JW, Courchesne E, Press GA, Yeung-Courchesne R, Hesselink JR (1989) Reduced cerebellar hemisphere size and its relationship to vermal hypoplasia in autism. *Arch Neurol* 46:689–694
27. Nopoulos PC, Ceilley JW, Gailis EA, Andreasen NC (1999) An MRI study of cerebellar vermis morphology in patients with schizophrenia: evidence in support of the cognitive dysmetria concept. *Biol Psychiatry* 46:703–711
28. Pulu G, Romero R, Reece EA, Goldstein I, Hobbins JC, Bovicelli L (1988) Subnormal cerebellum in fetuses with spina bifida. *Am J Obstet Gynecol* 158:1052–1056
29. Piven J, Saliba K, Bailey J, Arndt S (1997) An MRI study of autism: the cerebellum revisited. *Neurology* 49:546–551
30. Raz N, Torres IJ, Spencer WD, White K, Acker JD (1992) Age-related regional differences in cerebellar vermis observed in vivo. *Arch Neurol* 49:412–416
31. Raz N, Dupuis JH, Briggs SD, McGavran C, Acker JD (1998) Differential effects of age and sex on the cerebellar hemispheres and the vermis: a prospective MR study. *Am J Neuroradiol* 19:65–71
32. Roche AF, Mukherjee D, Guo SM, Moore WM (1987) Head circumference reference data: birth to 18 years. *Pediatrics* 79:706–712
33. Saitoh O, Courchesne E, Egaas B, Lincoln AJ, Schreibman L (1995) Cross-sectional area of the posterior hippocampus in autistic patients with cerebellar and corpus callosum abnormalities. *Neurology* 45:317–324
34. Schmahmann JD (2000) *MRI atlas of the human cerebellum*. Academic, San Diego, CA
35. Schmitt JE, Eliez S, Warsofsky IS, Bellugi U, Reiss AL (2001) Enlarged cerebellar vermis in Williams syndrome. *J Psychiatr Res* 35:225–229
36. Sener RN (1995) Cerebellar agenesis versus vanishing cerebellum in Chiari II malformation. *Comput Med Imaging Graph* 19:491–494
37. Shah SA, Doraiswamy PM, Husain MM, Figiel GS, Boyko OB, McDonald WM, Ellinwood EH, Krishnan KRR (1991) Assessment of posterior fossa structures with midsagittal MRI: the effects of age. *Neurobiol Aging* 12:371–374
38. SPSS (2001) *Statistical package for the social sciences for windows*. SPSS, Chicago, IL
39. Tsai T, Bookstein FL, Levey E, Kinsman SL (2002) Chiari-II malformation: a biometric analysis. *Eur J Pediatr Surg* 12(Suppl 1):S12–S18
40. Van Allen MI, Kalousek DK, Chernoff GF, Juriloff D, Harris M, McGillivray BC, Yong S, Langlois S, MacLeod PM, Chitayat D, Friedman JM, Wilson RD, McFadden D, Pantzar J, Ritchie S, Hall JG (1993) Evidence for multi-site closure of the neural tube in humans. *Am J Med Genet* 47:723–743
41. Variend S, Emery JL (1973) The weight of the cerebellum in children with myelomeningocele. *Dev Med Child Neurol* 15(Suppl 29):77–83